Robotics and Autonomous Systems 92 (2017) 152–161

Contents lists available at ScienceDirect

Robotics and Autonomous Systems

journal homepage: www.elsevier.com/locate/robot

Velocity-Based Robotic Assistance for Refining Motor Skill Training in a Complex Target-Hitting Task Using a Bio-Mimetic Trajectory Generation Model: A Pilot Study

Yoshiyuki Tanaka[1]

1-14 Bunkyo-machi, Nagasaki

Graudate School of Engineering, Nagasaki University[1,]*

Abstract

Several methods have been proposed for robotic assistance in motor learning/training. However, a few major concerns such as the design of the natural motion of the hand of a trainee/patient by a robotic device considering the motor ability of the trainee/patient and a safe and effective method for teaching a trainee/patient, especially in a complex task requiring motor timing, still need to be addressed. This paper proposes velocity-based robotic assistance (VRA) using a bio-mimetic trajectory generation model for motor skill training in a target-hitting task considering the concerns mentioned above. In the designed motor task, a trainee has to contact an approaching ball with a racket at the desired time to hit the target on the wall while predicting the behavior of the ball before and after the contact. A set of the racket angle and hand velocity at the contact time is defined as a task-related motor skill. In the motor training with VRA, the time scale of a primitive reference velocity profile is automatically adapted to individual levels of task-related motor skills recorded in the past trials with no robotic assistance. The robotic device then teaches the trainee the customized reference velocity profile to facilitate motor skill training. The effect of VRA on motor skill training in a target-hitting task was investigated with sixteen healthy volunteers (male university students aged 22-24 years) to verify the concept in this pilot study. The skilled hand movement for the designed motor task was first determined using a set of results measured from four skilled subjects, and the primitive reference velocity profile with multiple peaks was successfully regenerated in a minimum-jerk model by utilizing the task-related constraints. Next, a set of training experiments with and without VRA was conducted with twelve subjects who have no experience in the target task. The results for the healthy subjects of this pilot study demonstrated that the proposed VRA was efficacious in facilitating the acquisition of task-related motor skills (with almost half trials) and in reducing temporal errors of the desired velocity (by approximately 40 %).

Keywords: Robotic assistance, motor skill training, trajectory generation, individual adaptation

1. Introduction

Robotic assistance (RA) has been studied as an advanced technology to facilitate human motor training/learning by novice trainees for acquiring motor task skills and the recovery of motor functions in patients with motor disorders. The key steps in designing the RA system (RAS) include the generation of a reference motion for target tasks and teaching trainees/patients the designed reference motion according to their individual differences [1].

The reference trajectory for a target motor task is usually designed using the average motion of the skilled subjects recorded during preliminary tests. For the task in which the desired motion can be regarded as a primitive motion, i.e., a point-to-point reaching movement with a bell-shaped velocity pro-

*Yoshiyuki Tanaka

Email address: ytnk@nagasaki-u.ac.jp (Graudate School of Engineering, Nagasaki University)

http://dx.doi.org/10.1016/j.robot.2017.03.010

file [2], a computational bio-mimetic model for human trajectory generation, such as the minimum-jerk model [3], minimum-torque-change model [4], and time-based generator model [5, 6, 7], can be utilized for producing a family of reference trajectories depending on the task conditions including the movement time and the traveling length [8, 9, 10, 11]. However, in the case where the desired motion for a target task cannot be represented by the simple primitive motion, most of the RASs provide a recorded average motion of the skilled subjects as the sole reference trajectory for training. This would reduce the flexibility and effectiveness of the motor training/rehabilitation of trainees/patients [12, 13, 14]. A few RASs employ a computational bio-mimetic model to regenerate a complicated reference movement observed in a complex task. For example, Tanaka developed a RAS by using a minimum-jerk model refined for generating a reference profile having a smooth velocity with multiple peaks observed in a virtual curling task and demonstrated the effects of the RAS on motor skill learning by using the training results of healthy subjects [15]. However, the RAS designed for the virtual curling task did not consider the differences between the trainees to adapt to the reference motion, and the effects tend to depend on the individual motor skills of a trainee.

Further, the assist-as-needed strategy is often used in motor training/rehabilitation by RASs adapting to individual motor skills [16, 17]. In this control strategy, the robotic device provides an additional force to the reference motion according to the spatial and/or velocity errors so that a human operator can gradually generate the reference motion independently. Several studies reported the positive effects of this strategy on motor training/rehabilitation, especially for novice trainees in the early stages of motor training [18, 19]. However, the reference motion is basically limited to a simple primitive motion.

Thus, generating the desired natural motion of the hand of a trainee/patient in such a complex task, regulating the motion with respect to the motor ability of the trainee/patient, and teaching trainees/patients the individual desired motion as safely and effectively as possible are considerable issues yet to be addressed.

In this paper, as an example for performing complex motor tasks using complicated movements, a velocity-based RA (VRA) methodology is proposed for a target-hitting task that requires timing. The methodology utilizes a biological computational model for generating a hand trajectory relative to the target task and adapts the reference motion to the level of the motor skills of the operator. The primary aim of this pilot study is to verify the concept of the proposed VRA.

The remainder of this paper is organized as follows. Section 2 describes the hardware of a robotic manipulandum system and the model of the target-hitting task. Section 3 defines the reference motion for the motor task according to the preliminary tests of the skilled subjects and presents the computational model with task-related constraints for generating a reference trajectory considering the behavioral timing. An adaptation algorithm of the reference trajectory in the proposed VRA system is then explained in detail. In Section 4, a set of experimental results shows that the healthy subjects improved their scored points and motor skills related to the target-hitting task as motor learning progressed. Further, it is verified that the proposed VRA is effective in improving motor learning for generating the desired velocity profile until the impact of the ball.

2. Robotic System for Motor Skill Training in Target-Hitting Task

2.1. Hardware Structure

Fig. 1 shows the robotic manipulandum system developed to train motor skills of the upper limb of a trainee in a target-hitting task, named "Virtual Tennis". A human operator stands in front of the robotic system and manipulates the handle to strike an approaching ball using a racket and hit the center of the target circle on a wall in the virtual space according to the visual biofeedback display.

The robotic manipulandum has two linear motor tables each with one degree of freedom placed orthogonally to allow the motion of the hand in the horizontal plane. The hand force generated by an operator is measured using a six-axis force/torque sensor attached to the handle of the robot, and the position of the hand is determined using encoders built in the linear motor tables [15]. The motion of the handle is controlled using an impedance control method [20]:

$$\boldsymbol{F}_e = \boldsymbol{M}_r \ddot{\boldsymbol{X}}_e + \boldsymbol{B}_r \dot{\boldsymbol{X}}_e \tag{1}$$

where $\boldsymbol{F}_e = (F_{ex}, F_{ey})$, $\boldsymbol{X}_e = (X_{ex}, X_{ey}) \in \Re^2$, $\boldsymbol{M}_r = \mathrm{diag.}(m_r, m_r)$, $\boldsymbol{B}_r = \mathrm{diag.}(b_r, b_r) \in \Re^{2\times 2}$

http://dx.doi.org/10.1016/j.robot.2017.03.010

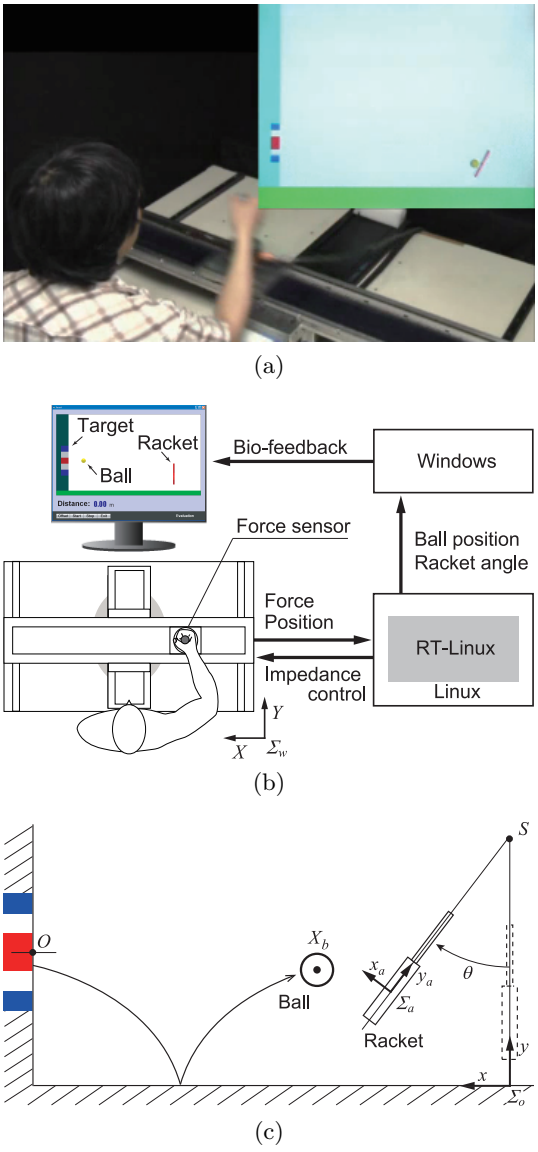

Figure 1: An overview of the robotic manipulandum system developed for a target-hitting task. (a) A subject stands in front of the system and manipulates the handle so that the ball hit by the racket bounced back to the center of the target on the wall. (b) The system is composed of a robotic device to provide virtual force loads to the hand of an operator. (c) The ball is thrown from the center of the target with a certain velocity and fell freely, whereas the racket rotates around a fixed point according to the hand motion.

denote the hand force, hand position, inertia of the robot handle, and viscosity, respectively, and the origin of the world coordinate system Σ_w is set at the initial position of the handle. Moreover, the robotic system can teach the operators a certain reference hand motion $\boldsymbol{X}_r = (X_{rx}, X_{ry}) \in \Re^2$ to hit the center of the target circle by utilizing a PID controller, which controls the handle of the robotic device.

The hand motion for the target-hitting task was allowed along the X direction in this pilot study, in which the hand force along the Y direction F_{ey} was eliminated when the manipulandum system was controlled. Accordingly, the rest part of this paper discusses the hand motion along the X direction.

2.2. Model of Target-Hitting Task

Fig. 1(c) illustrates the model of the target-hitting task. A ball of radius r_b is thrown from a certain point with the specified initial velocity toward a racket, whereas the racket is rotated around a fixed point $\boldsymbol{S} = (S_x, S_y) \in \Re^2$ according to the position of the hand along the x-axis X_{ex}. The angle of the racket θ is synchronized with the position of the hand as $\theta = \frac{5\pi}{4} X_{ex}$.

The motion of the ball before contacting the racket is given by

$$\begin{cases} M_b \ddot{X}_{bx} = 0 \\ M_b \ddot{X}_{by} = -\frac{1}{2} M_b g \end{cases} \tag{2}$$

where $\boldsymbol{X}_b = (X_{bx}, X_{by}) \in \Re^2$ is the position of the ball, M_b is the inertia of the ball, and g is the gravitational acceleration. The behavior of the ball after contacting the racket is then calculated by setting the following ball velocity just after the impact of the ball $\dot{\boldsymbol{X}}_b^* = (\dot{X}_{bx}^*, \dot{X}_{by}^*) \in \Re^2$ in Eq. (2) as

$${}^o\dot{\boldsymbol{X}}_b^* = {}^o\boldsymbol{R}_a(\theta^*)\, {}^a\dot{\boldsymbol{X}}_b^* \tag{3}$$

with

$$\begin{cases} {}^a\dot{X}_{bx}^* = \frac{5\pi}{4} {}^aS_y v^* \\ \qquad\qquad + e_{br}\left(\frac{5\pi}{4} {}^aS_y v^* - {}^a\dot{X}_{bx}(t_c)\right) \\ {}^a\dot{X}_{by}^* = {}^a\dot{X}_{by}(t_c) \end{cases} \tag{4}$$

where ${}^o\boldsymbol{R}_a(\theta) \in \Re^{2\times 2}$is the rotation matrix transformed from the basic coordinate system Σ_o to the local coordinate system attached at the impact point Σ_a, e_{br} is the coefficient of restitution between the ball and the racket, t_c is the contact time, and θ^* and v^* are the racket angle and hand velocity on ball impact, i.e., $\theta(t_c)$ and $v(t_c)$, respectively.

In the target task, a point is scored corresponding to the distance e_p between the ball hitting position

http://dx.doi.org/10.1016/j.robot.2017.03.010

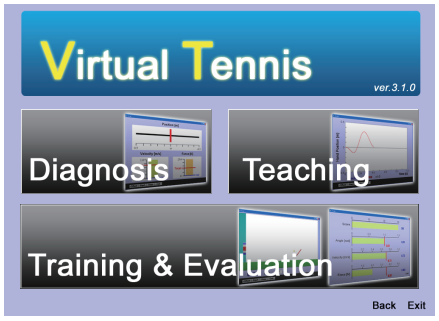

(a)

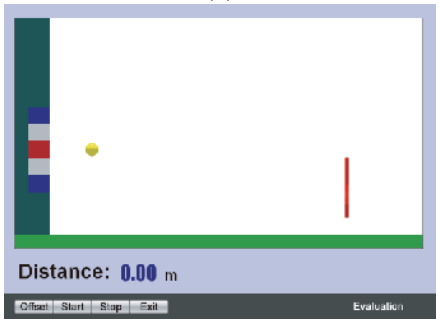

(b)

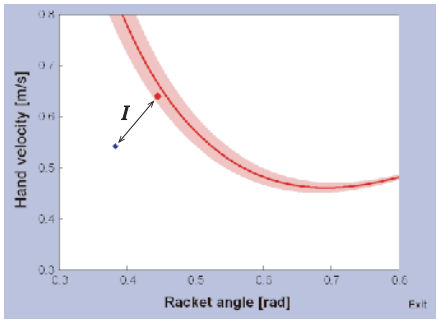

(c)

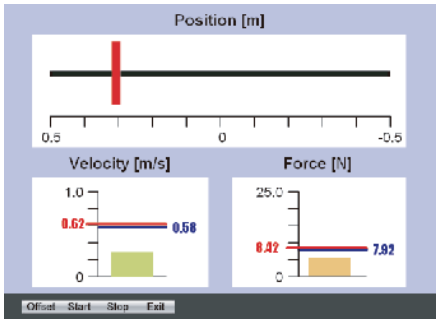

(d)

Figure 2: Images of GUI for motor training in the target-hitting task. (a) The panel of the main menu. (b) The initial situation of the target-hitting task. (c) The evaluation of task-related skill showing in the training & evaluation mode. (d) The diagnosis of motor ability in hand motion.

on the wall and the center of the target $\boldsymbol{O} = (o_x, o_y) \in \Re^2$ that can be calculated from the task model as

$$e_p = \Big| o_y + \frac{g}{4(\dot{X}^*_{bx})^2}\left(o_x - r_b - X_{bx}(t_c)\right)^2 - \frac{\dot{X}^*_{by}}{\dot{X}^*_{bx}}\left(o_x - r_b - X_{bx}(t_c)\right) - X_{by}(t_c) \Big|, \tag{5}$$

where r_b is the radius of the ball. The distance e_p is controlled by both the racket angle θ^* and hand velocity v^* at the contact. Accordingly, in this study, the task-related skill is defined by (θ^*, v^*).

2.3. Graphic User Interface for Motor Skill Training

Fig. 2 illustrates an interactive graphic user interface (GUI) system for motor skill training integrated into the developed robotic manipulandum. Fig. 2(a) presents the main panel for providing three training modes in the developed system: the teaching mode, the training & evaluation mode, and the diagnosis modes. Fig. 2(b) shows the initial setting of the target-hitting task. Fig. 2(c) shows the visual feedback information indicating the task-related skills of a trainee. Fig. 2(d) shows the diagnosis of the motor capabilities of a trainee in reaching movements.

The teaching mode is used to teach a trainee/patient a reference hand motion that is designed according to the level of the task-related skills of the trainee/patient. In this mode, the hand can follow the reference motion by RA. In the training & evaluation mode, a trainee conducts the target task with his efforts and no RA is provided to his hand motions, and the evaluation of the task-related skill is presented on another window after every trial. In the diagnosis mode, the robotic system evaluates the maximum hand force, hand velocity, and range of hand motion during free manipulation of the handle by the trainee. The diagnosis result can be utilized to determine the specification of an initial reference motion according to each trainees/patient.

Fig. 3 illustrates a typical scheme of the three modes for motor skill training, but the practical scheme for a trainee/patient should be decided after consulting a therapeutist about the condition of the trainee/patient.

2.4. Parameter setting

The values of the parameters for the impedance control of the robot and task model were determined according to the experimental specifications

http://dx.doi.org/10.1016/j.robot.2017.03.010

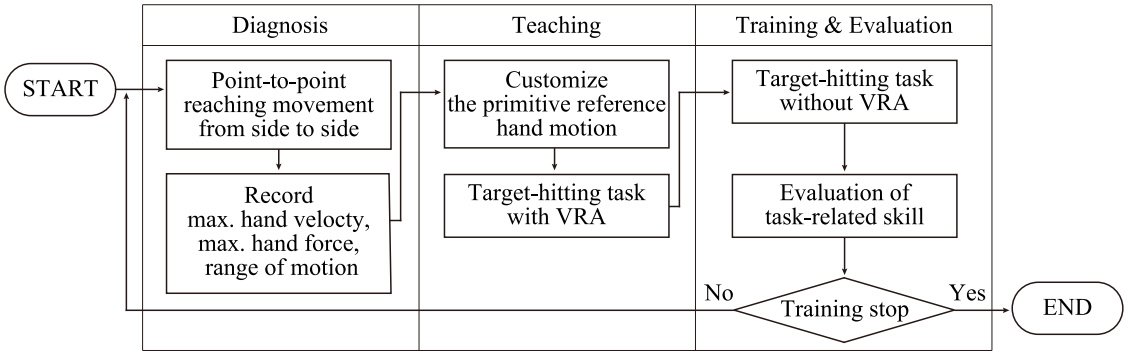

Figure 3: A typical block scheme of the three modes in the developed VRA system.

as follows. The impedance parameter of the robot was set at $(m_r, b_r) = (5.0\ \text{kg}, 5.0\ \text{Ns/m})$, the initial position of the ball at $\boldsymbol{X}_b(0) = (3.0\ \text{m}, 1.0\ \text{m})$, the initial velocity of the ball at $\dot{\boldsymbol{X}}_b(0) = (-1.5\ \text{m/s}, 1.5\ \text{m/s})$, the moment of inertia of the ball at $M_b = 0.25$ kg, the radius of the ball at $r_b = 7.5$ cm, the center of the target circle at $\boldsymbol{O} = (3.5\ \text{m}, 1.0\ \text{m})$, and the coefficient of restitution between the ball and racket at 0.8.

Points were obtained according to the distance e_p between the center of the target and the hitting point on the wall. Ten points for less than 0.1 m, 8 points for less than 0.2 m, 6 points for less than 0.3 m, 4 points for less than 0.4 m, and 2 points for less than 0.5 m. No points were recorded when e_p was greater than 0.5 m and when the ball hit the ground before hitting the wall.

3. VRA with Individual Adaptation

3.1. Reference motion in Target-Hitting Task

The hand motion of skilled subjects who can control their hand movements appropriately to score higher points can be used as a reference motion to train novices. To determine such skilled motion of the hand, a set of measurement tests was conducted for four skilled subjects (Subs. I-IV). In the training experiment, the subjects were asked to stand in front of the display and hit the target with a ball using their dominant hand (right hand) freely without any RA. During the preparation tests, they repeated the task for an adequate number of trials (approximately 100 trials) until they acquired the skill of constantly returning the ball to the center of the target. Then they performed a set of 40 trials to determine a trained hand motion for this task.

Fig. 4 shows the results of the tests conducted with skilled subjects. Fig. 4(a) illustrates the relationship between the score (e_p) and the task-related skill for Sub. I, and the map was plotted by using Eq. (5). The subject scored points stably although some deviations were observed in the points. Fig. 4(b) shows the process of scoring points by the skilled subjects according to the trial number. In the figure, the bottom of each box is the 25th percentile of the mean score for the skilled subjects, the top is the 75th percentile, the black line in the middle is the 50th percentile, and the whisker represents the upper and lower adjacent values. The skilled subjects scored better points stably because of the preliminary training sets. Fig. 4(c) shows the averaged hand velocity profile corresponding to ten points scored by the four subjects using the solid line in which the shaded area represents the standard deviations of the measured velocity profiles. The initial time of the hand movement t_0 was determined when the velocity of the hand was greater than 0.001 m/s, the end time of the backswing was recorded at the first change in the sign of the velocity, and the terminal time t_f was determined when the velocity of the hand was lesser than 5 % of the maximum value in each trial. The contact time t_c and the time at peak velocity t_p were determined using the processed data of the ball and hand movements. The desired task-related skill at the contact time was calculated as $(\Theta_d^*, V_d^*) = (0.550\ \text{rad}, 0.516\ \text{m/s})$. The skilled velocity profile for the target task is observed as a smooth wave with one peak and two concaves.

Remarkably, the subjects generated almost the same velocity profile until the impact of the ball because of smaller individual differences. This sug-

http://dx.doi.org/10.1016/j.robot.2017.03.010

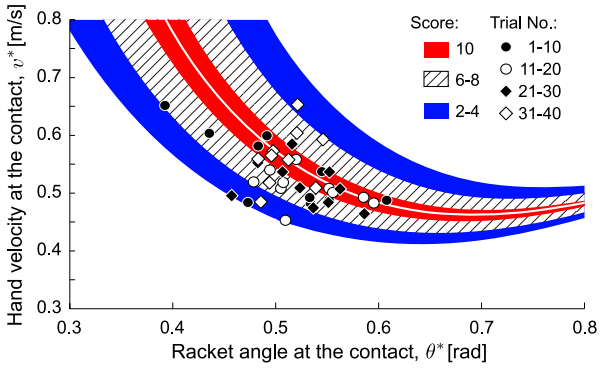

(a)

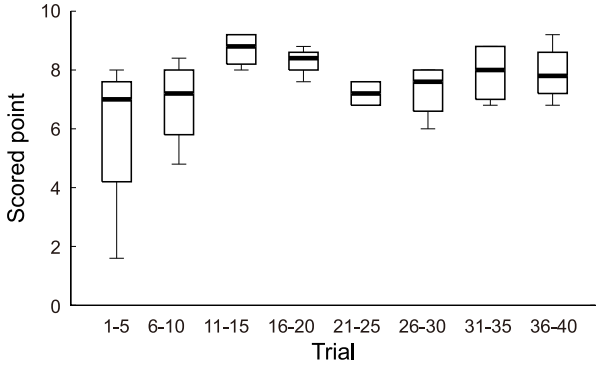

(b)

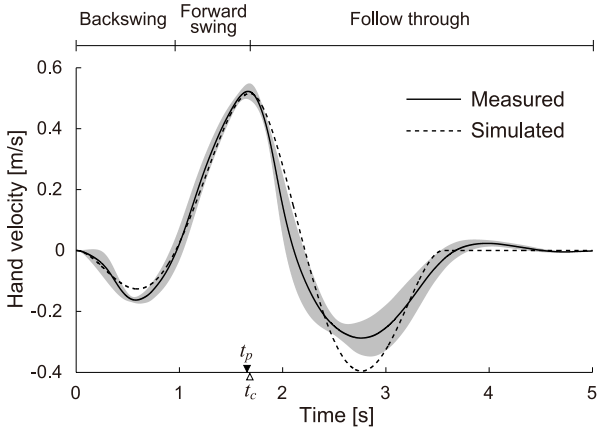

(c)

Figure 4: Typical results of the scored points and task-related skills and the averaged hand velocity profile by the skilled subjects. (a) The map of scored points according to racket angle and hand velocity at the contact time. (b) The box plot of scored points for the skilled subjects according to the trial number. (c) The mean profile of hand velocities measured in the case where the skilled subject scored 10 points (the solid line) and the simulated velocity profile (the broken line).

gests that the smooth hand motions during the backward and forward swings are extremely important in the target-hitting task, and the hand motions should be carefully provided during training with RA. Furthermore, the time of peak velocity t_p almost agrees with the contact time t_c as observed in other motor tasks requiring precise timing, such as a freefall ball catching task [21, 22, 23] and a ball punching task [24, 25, 26]. Thus, the subjects required motor timing to contact the approaching ball in addition to hitting the target on the wall; the designed task is more difficult and complex than the conventional point-to-point reaching and interception tasks.

3.2. Bio-Mimetic Trajectory Generation with Task-Related Constraints

The reference motion along the X direction in the target-hitting task is computed in the framework of a minimum-jerk model [3] by using a cost function J given by

$$J = \frac{1}{2}\int_0^{t_f} \left\{ \dddot{X}_{rx} \right\}^2 dt \tag{6}$$

with the task-related constraints at the initial time of the hand motion t_0, the contact (ball hitting) time t_c, and the terminal time of the hand motion t_f as follows:

$$\begin{cases} (X_{rx}(t_0), \dot{X}_{rx}(t_0), \ddot{X}_{rx}(t_0)) = (X_0, 0, 0) \\ (X_{rx}(t_c), \dot{X}_{rx}(t_c), \ddot{X}_{rx}(t_c)) = (\frac{4}{5\pi}\Theta_d^*, V_d^*, 0) \\ (X_{rx}(t_f), \dot{X}_{rx}(t_f), \ddot{X}_{rx}(t_f)) = (X_f, 0, 0) \end{cases} \tag{7}$$

where the hand positions at t_0 and t_f are set as $X_0 = X_f = 0$ in this study. This bio-mimetic model for trajectory generation can regenerate the skilled hand movement by solving the aforementioned differential equations using a pseudo-Newton method in which the values of the constraint parameters are based on the hand movements of the skilled subjects (see Appendix).

Fig. 4(c) presents the simulated velocity profile (the broken line) for the desired target task-related skill $(\Theta_d^*, V_d^*) = (0.550 \text{ rad}, 0.516 \text{ m/s})$ in which the periods for the task-related constraints were set as $t_c = 1.683$ s and $t_f = 3.555$ s. The simulated velocity profile agrees with the measured average profile, and it can be employed as the primitive reference motion in VRA for motor skill training in the task.

3.3. Individual Adaptation of Primitive Reference in Training

The primitive reference motion is utilized in VRA for teaching a trainee the desired motion; however,

http://dx.doi.org/10.1016/j.robot.2017.03.010

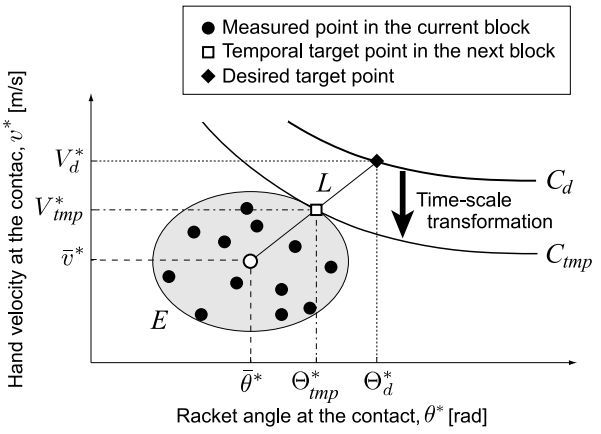

Figure 5: Illustration of an algorithm for adapting the primitive reference trajectory in training with VRA. Both peak and duration of the reference velocity profile are designed based on the measured data of task-related skill in the past trials by means of time scale transformation technique.

it may be difficult for some novices to learn the desired target-related skill (Θ_d^*, V_d^*) and regenerate the primitive reference because of its motion speed, task difficulty, and motor abilities of the trainee. To cope with such individual capabilities, in this study, the primitive reference velocity profile is adapted in the task-related skill (θ_d^*, v_d^*) for each trainee according to the training data recorded in the previous trials using the time scale transformation technique, as shown in Fig. 5.

A task-skill ellipse E is formulated as

$$\frac{(\theta^* - \bar{\theta}^*)^2}{r_\theta^2} + \frac{(v^* - \bar{v}^*)^2}{r_v^2} = 1 \tag{8}$$

where the center of the ellipse ($\bar{\theta}^*$, $\bar{v}^*$) is the averaged task-related skill in a block of a few trials, and r_j ($j \in \{\theta, v\}$) is the regulation parameter calculated by the following Gaussian function using the standard deviations σ_j as,

$$r_j = r_j^{max} - (r_j^{max} - r_j^{min}) \exp\left\{-\frac{(\sigma_j - \alpha)^2}{2\beta^2}\right\} \tag{9}$$

where r_j^{max} and r_j^{min} are the maximum and minimum values of r_j, respectively, and α and β are constants.

The individual temporal target of the task-related skill (Θ_{tmp}^*, V_{tmp}^*) is defined as the crossing point of ellipse E and line L connecting the center of ellipse E and the desired target skill (Θ_d^*, V_d^*) located on the curve for the 10 points C_d. As the temporal target velocity V_{tmp}^* differs from the hand velocity required to hit the ball at the center of the target, the curve C_d has to be shifted to an appropriate curve C_{tmp} that includes the temporal target point ($\Theta_{tmp}^*, V_{tmp}^*$) for scoring the 10 points. To solve this problem, the time scale transformation technique is utilized to regulate the speed of the ball in the virtual task space [27]. The relationship between the actual time t and the virtual time ν is given by

$$c = \frac{d\nu}{dt} = \frac{V_{tmp}^*}{\tilde{V}_{tmp}^*} \tag{10}$$

where $c > 0$ is the time scale constant and $\tilde{V}_{tmp}^*$ is the temporal target of the hand velocity required to hit the ball at the center of the target according to the racket angle Θ_{tmp}^* in the virtual time axis. Note that the moving speed of the ball reduces when the value of c is less than 1.0.

Transforming the time scale of the target-hitting space from the actual time t to the virtual time ν, the ball velocity just after the impact of the ball is given by

$$\frac{d^o \boldsymbol{X}_b^*}{d\nu} = {}^o\boldsymbol{R}_a(\theta) \frac{d^a \boldsymbol{X}_b^*}{d\nu} \tag{11}$$

$$\begin{cases} \frac{d^a X_{bx}^*}{d\nu} = {}^a S_y \dot{\theta}_\nu + e_{br}\left({}^a S_y \dot{\theta}_\nu - \left.\frac{d^a X_{bx}}{d\nu}\right|_{\nu=\nu_1}\right) \\ \frac{d^a X_{by}^*}{d\nu} = \left.\frac{d^a X_{by}}{d\nu}\right|_{\nu=\nu_1} \end{cases}$$

where ν_c and $\dot{\theta}_\nu$ are given as follows:

$$\nu_c = \frac{t_c}{c}, \tag{12}$$

$$\dot{\theta}_\nu = \frac{1}{c}\dot{\theta} = \frac{1}{c}\frac{5}{4}\pi \dot{X}_e(\nu_c). \tag{13}$$

The moving speed of the ball is inversely proportional to the value of c. When the hand velocity during the impact of the ball is V_{tmp}^*, and Eq. (13) is also converted to

$$\dot{\theta}_\nu = \frac{5}{4}\pi \tilde{V}_{tmp}^*. \tag{14}$$

Thus, the trainee can hit the ball at the center of the target by generating the hand velocity V_{tmp}^* according to the racket angle Θ_{tmp}^* during the impact of the ball.

http://dx.doi.org/10.1016/j.robot.2017.03.010

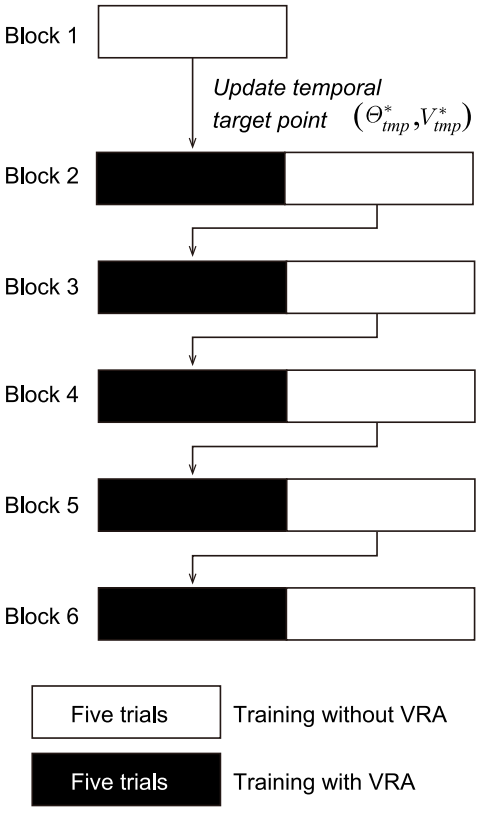

Figure 6: An outline of the experimental protocol using the developed system for GI. A trainee carries out the task by himself in the training mode, whereas the trainee learns the desired hand motion in the teaching mode provided by VRA.

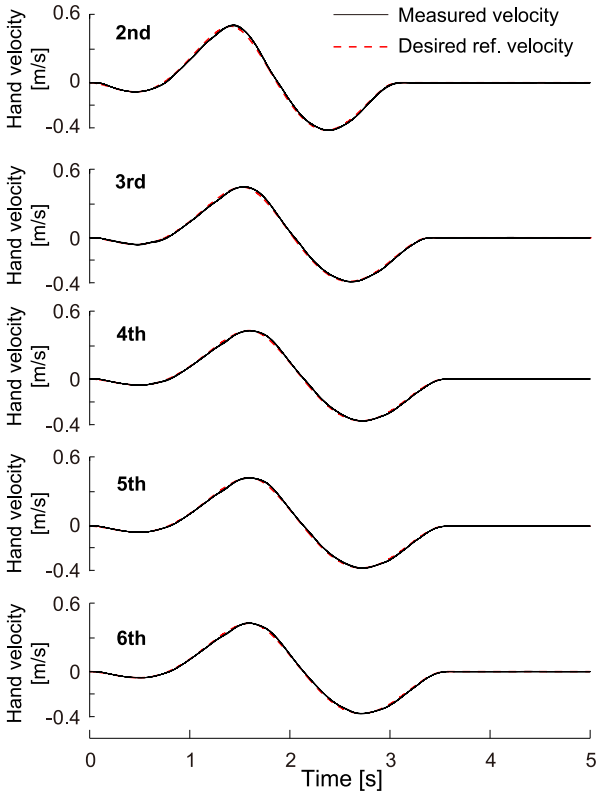

Figure 7: Time profiles of the hand (handle) velocity for five trials in the teaching mode by VRA. The robot handle precisely tracked the desired velocity profile by means of the PID controller.

4. Training Experiments

4.1. Procedure

Twelve healthy volunteers (male university students aged 22-24 years) participated in this study. They were briefed about the aim of the research and target-hitting task, and sets of motor skill training with and without VRA were tested. The handle of the robot followed the primitive/regulated reference trajectory to teach the trainees the skillful hand motion in training with VRA.

The subjects were divided into two groups with or without VRA. Five subjects (Subs. A-E) of the first group (GI) performed five sets composed of five trials with VRA and another five trials without VRA after the initial five trials without VRA (i.e., total 55 trials) as shown in Fig. 6. Seven subjects (Subs. F-L) of the second group (GII) performed the same number of trials without VRA. In each of the trials with VRA for GI, the reference motion (time scale constant) was updated according to the data of the task-related skill recorded in the past five trials without VRA (See Fig. 6).

The desired target point (Θ^*_d, V^*_d) was set at (0.7 rad, 0.461 m/s), which is the different point on the curve C_d from the point obtained in the skilled subjects, in order to investigate the effectiveness of the proposed VRA on motor skill learning in the target-hitting task.

The effects of VRA on the motor skill acquisition for the target-hitting task were then investigated using the following two quantitative indices: the task-related skill I and the velocity profile errors to the primitive reference before ball contact RMSE (root-mean-square-error).

$$I = ||(\Theta^*_d, V^*_d) - (\bar{\theta}^*, \bar{v}^*)||, \tag{15}$$

$$\mathrm{RMSE} = \sqrt{\sum_{i=0}^{N} \frac{(v_{ref}(i) - v(i))^2}{N}}, \tag{16}$$

where i is the sample number and N is the number of sampled data.

http://dx.doi.org/10.1016/j.robot.2017.03.010

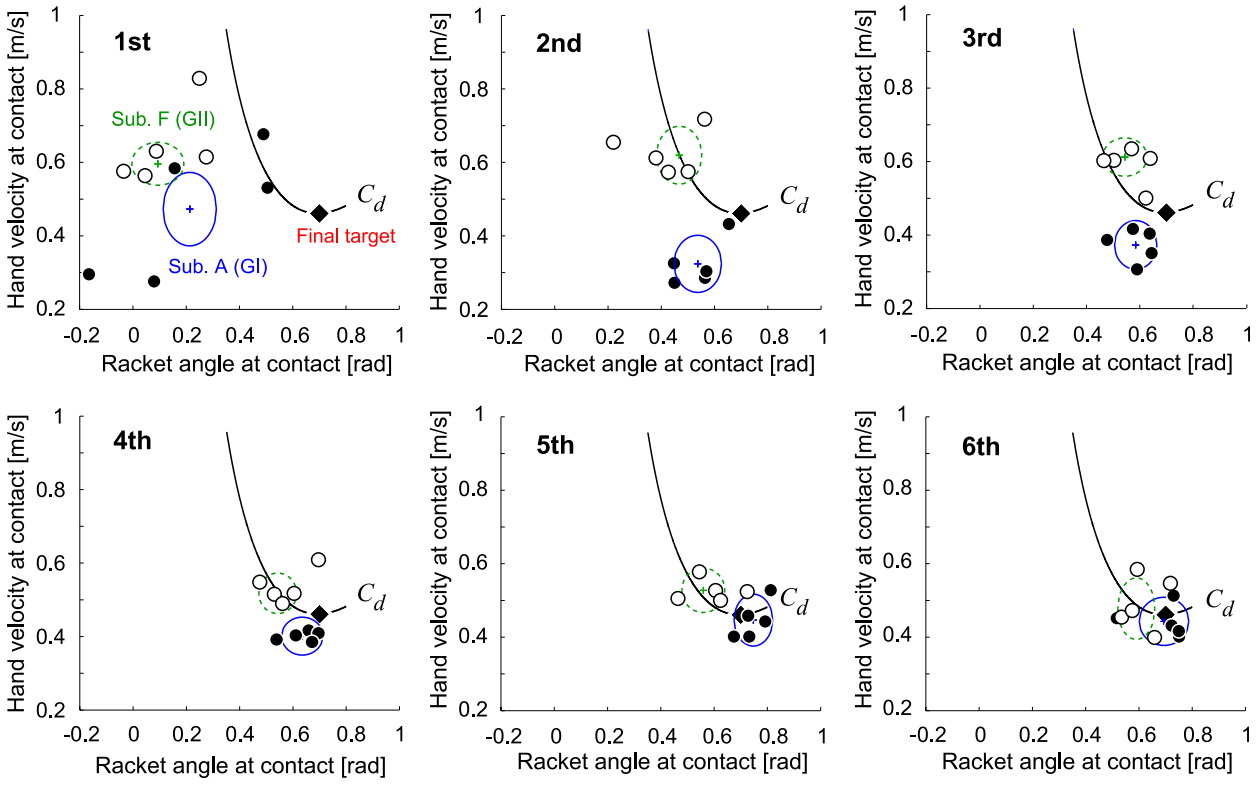

Figure 8: Processes of motor skill learning with and without VRA. A circle and a closed diamond represent the points of the task-related skill measured and the desired target point (0.7 rad, 0.461 m/s), respectively. The closed circles tend to locate near the diamond in the results for Sub. A (GI) with the progress of the blocks.

Table 1: Changes of the time scale constant, c, in training with VRA.

Block	2	3	4	5	6
Sub. A	0.664	0.665	0.896	0.969	1
Sub. B	0.978	0.980	1.048	1.046	1.082
Sub. C	1.138	1	1	1	1
Sub. D	1.049	1.027	1.023	1.006	1
Sub. E	1.224	1.046	1.002	1	1

A Wilcox t-test was conducted to compare the values of the scored points, task-related skills, and RMSEs between the two groups in R [28]. A multiple comparison test (Bonferroni correction) was also conducted for those values according to the block number.

4.2. Experimental Results

Table 1 lists the changes in the time scale constant c that was utilized in the teaching trials with VRA for GI. The reference motion was regulated according to the level of task-related skills of each subject by means of the time scale transformation. Fig. 7 presents the time profiles of the hand velocities for five trials (a black solid line) with the regulated reference velocity (a red broken line) in the teaching mode by VRA according to the block number. It can be observed that the training system successfully traced the reference velocity profiles in the experiments.

Figs. 8 and 9 illustrate the training results of Sub. A (GI) and Sub. F (GII). Fig. 8 presents the changes in the task-related skills (θ^*, v^*). In the figure, the diamond indicates the final target point relative to the desired task-related skill, the circle represents the point of the task-related skill measured in each trial, and the cross mark is the center point of the task-skill ellipse E in each block. In the first block, the skills of Subs. A and F were far from the final target point with large dispersions. With the progress in the number of blocks, the skills of Sub. A smoothly converged with the final target point (0.7 rad, 0.461 m/s) to score higher points

http://dx.doi.org/10.1016/j.robot.2017.03.010

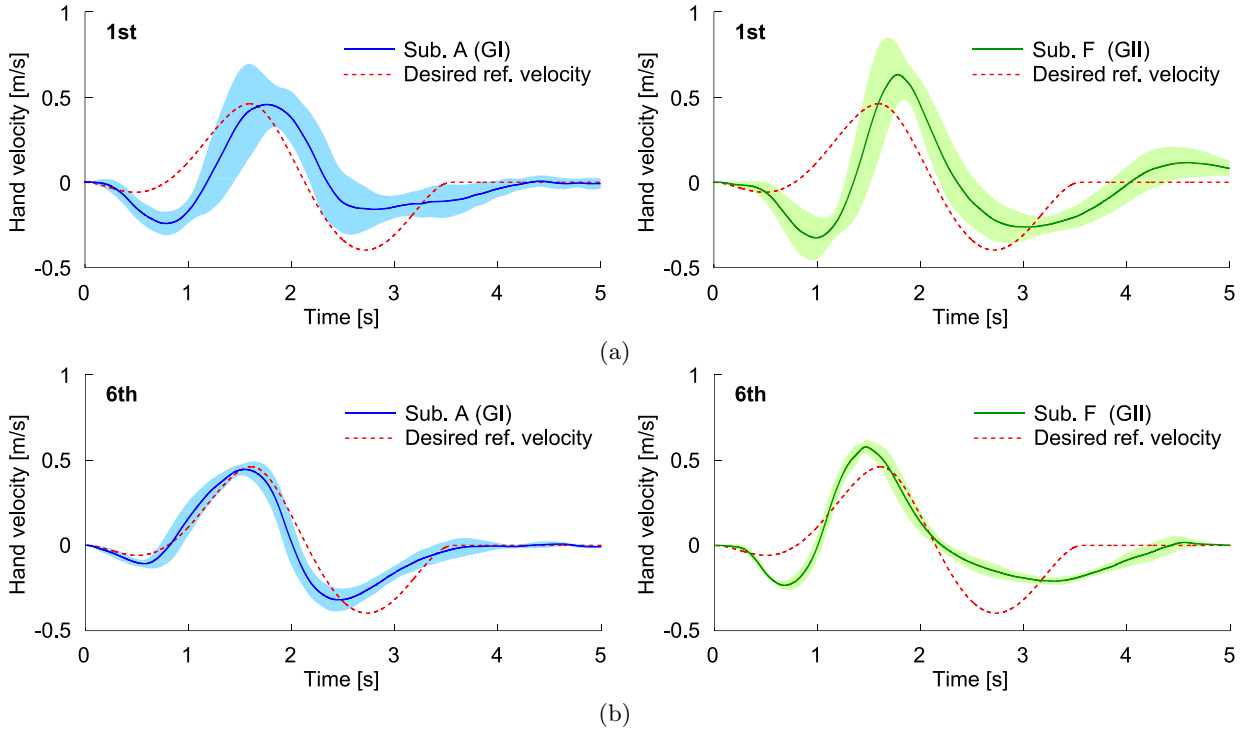

Figure 9: Hand velocity profiles with and without VRA in the first and sixth blocks. The solid line and the broken line represent the mean of velocity profiles and the desired velocity profile, respectively, and the shade represents the standard deviation.

Table 2: Statistical results of the multiple comparison tests according to the blocks.

	Pair of blocks	1-2	1-3	1-4	1-5	1-6	2-6
GI	Scored point			*			
	Task-skill index	*	**	**	**	**	
	RMSE	*	*	**	**	**	
GII	Scored point						
	Task-skill index		**	**	**	**	*
	RMSE			*	*	**	*

*: $p < 0.05$, **: $p < 0.01$

in the earlier block number, whereas the skills of Sub. F slowly but unstably converged with another point. Fig. 9 shows the averaged velocity profiles for Subs. A and F measured in the first block without VRA and in the last block, in which the shades represent the standard deviations of the profiles. Both the subjects were observed to generate almost unique velocity profiles in the last block, and the average profile for Sub. F obviously differs from the reference velocity profile for the final target point. Similar tendencies were observed in the results corresponding to the other subjects.

Fig. 10 shows the changes in the mean data of the scores recorded in the five trials without VRA for all the subjects. In addition, the values of index I and RMSE are shown in the top-to-bottom order. Table 2 presents the statistical results of the multiple comparison tests according to the block number in each group. It can be observed that the values of the task-skill index and RMSE were significantly decreased in both groups as increasing the block number.

The mean scores of both the groups tend to increase with an increase in the block number, as shown in Fig. 10(a). The mean score of GI was slightly more than that of GII in each block, but no significant differences were observed between the groups. However, significant differences were observed between the first and fourth block in GI ($p < 0.05$). Next, the mean value of the task-skill index of GI was lower than that of GII in each block, and significant differences were observed between the two groups in the second block ($p < 0.05$) and the last two blocks ($p < 0.02$ for the fifth block; $p < 0.05$ for the sixth block), as shown in Fig. 10(b). In addition, the mean value was significantly de-

http://dx.doi.org/10.1016/j.robot.2017.03.010

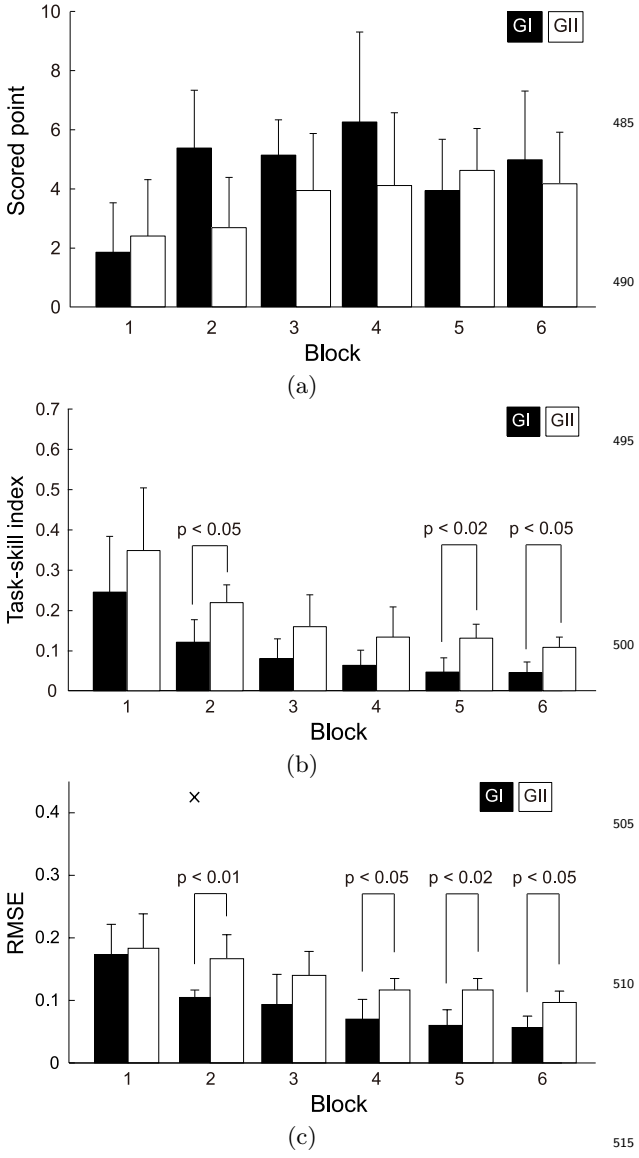

Figure 10: Comparison of the results of the scored points, task-related skill, and velocity error between the two groups. (a) The mean of average scores in each block, and the standard deviation. (b) The mean of average values of the evaluation index for task-related skill in each block, and the standard deviation. (c) The mean of RMSEs in each block and the standard deviation.

creased according to the block number in both the groups. This implies that the subjects in GI could hit the ball more precisely with the desired task-related skill (0.7 rad, 0.461 m/s) than the subjects in GII. Finally, the mean value of RMSE decreased in both the groups with an increase in the block number, as shown in Fig. 10(c), where the cross mark indicates the outlier which was detected in the data of GI in the second block by Smirnov- Grubbs test ($p = 0.000497$). The mean value was significantly decreased according to the block number in both the groups. Significant differences between the two groups were observed from the earlier blocks ($p < 0.01$ for the second block; $p < 0.05$ for the fourth block; $p < 0.02$ for the fifth block; $p < 0.05$ for the sixth block). In the final block, the mean value of GI was reduced by approximately 40 % compared to that of GII.

Consequently, the proposed VRA that uses a reference velocity profile adapted to the individual level of task-related skills was significantly effective in refining the temporal properties of the hand motion of a trainee/patient for the target-hitting task and in promoting the acquisition of the desired task-related skill.

5. Discussion and Conclusions

In this pilot study, a VRA was proposed using a biological computational model for generating a hand trajectory in the target-hitting task that requires timing. In the designed task, a trainee must contact an approaching ball with the desired task-related skill (racket angle and hand velocity) and hit the target on a wall while predicting the behavior of the ball before and after the contact. In motor training with VRA, the robotic manipulandum teaches the trainees a temporal reference hand motion that is determined by adapting a primitive reference motion to the individual task-related skills recorded in the previous trials without VRA.

The skilled hand movement was determined using a set of measured results of the skilled subjects. The primitive reference motion requiring VRA was then successfully regenerated in the framework of a minimum-jerk model with task-related constraints. This facilitated in continuously connecting two primitive movements before and after the ball contact. Next, training experiments with and without VRA were conducted for 12 healthy volunteers. The results of this study demonstrate that VRA significantly affected the motor skill training by improving the task-related skills and errors relative to the velocity profile until the ball contact. Furthermore, the acquisition of specified motor skills for the target-hitting task was expedited.

In the designed task, the trainees were required to have the ability to predict the behavior of the ball and the motor timing of the impact of the ball

http://dx.doi.org/10.1016/j.robot.2017.03.010

and generate a smooth velocity profile during discrete hand movement to hit the ball successfully on the target on the wall. On the basis of the internal model concept [29, 30, 31, 32], it can be supposed that the trainees formulated the internal model of the ball dynamics in their cerebellum during the process of motor learning by repeated trials, as mentioned in the reports of other interception tasks requiring precise timing (ex. [16, 22, 23]). Then they controlled the motor timing of the hand motion in their cerebrum by synchronizing a neural signal from the cerebellum [33]. Thus, the VRA may also be effective in training or refining such neural motor circuits in the central nervous system, although more detailed discussions relative to the internal model and motor learning strategies are required.

In conclusion, in this paper, VRA that uses a biomimetic trajectory generation model was proposed for motor skill training in a target-hitting task that required timing. The results of the training experiments with the twelve volunteers demonstrated that VRA significantly affected motor skill training. However, further investigations on the effects of the proposed VRA have to be carried out because the sample size of this pilot study was small and all volunteers who participated were young and healthy. It has been reported that age-related learning differences are robust in complex tasks but not absolute [34] and that the reaction times to visual stimuli are increased with age in a simple button-press task [35, 36]. Such evidences on age-related effects may suggest that the efficacy of motor skill training by VRA would be reduced because of a delay in the response of motion onset of the ball on display for the target-hitting task.

Thus, the future research will be directed to increase the number of subjects, including aged healthy volunteers as well as patients who have difficulty in controlling the motion of their limbs, especially for a movement task requiring precise timing, and investigate their training efficiency by comparing with other training approaches. Moreover, the mechanical impedance properties of the hand will be further examined according to the level of task-related skills, as well as task conditions such as the weight of the ball used in the test and the position of the target, to biomechanically evaluate the control ability of the neuromuscular dynamics of the arm in motion [21, 37, 38, 39].

Acknowledgment

The author greatly thanks to Mr. **Masataka Ishii** and Mr. **Haruhito Inoue** for their many contributions at Hiroshima University in this research work. This work was partly supported by JSPS KAKENHI (16760203, 18760193).

Appendix

For solving hand trajectory for target-hitting task with the constraints at the time t_c, the time scale t is transformed into τ $(0 \le \tau \le 1)$:

$$\tau = \begin{cases} t/T_1 & (0 \le t < t_c) \\ (t - T_1)/T_2 & (0 \le t \le t_f) \end{cases} \tag{17}$$

where T_1 and T_2 are time intervals given by

$$\begin{cases} T_1 = t_c \\ T_2 = t_f - T_1. \end{cases} \tag{18}$$

The vectors of control variables $\boldsymbol{u}$, state variables $\boldsymbol{x}$ and Lagrange multipliers $\boldsymbol{\lambda}$ are defined as

$$\boldsymbol{u} = [\delta_1, \delta_2]^T, \tag{19}$$

$$\boldsymbol{x} = [x_1, v_1, a_1, x_2, v_2, a_2]^T, \tag{20}$$

$$\boldsymbol{\lambda} = [\lambda_{x1}, \lambda_{v1}, \lambda_{a1}, \lambda_{x2}, \lambda_{v2}, \lambda_{a2}]^T \tag{21}$$

where x, v, a, and δ are the hand position, velocity, acceleration and jerk, respectively. Subscripts 1 and 2 represent the time intervals T_1 and T_2, respectively. Next, the equations of state are given by

$$\acute{\boldsymbol{x}} = [T_1 v_1, T_1 a_1, T_1 \delta_1, -T_2 v_2, -T_2 a_2, -T_2 \delta_2]^T \tag{22}$$

where $(\acute{})$ represents the derivative by time τ.

The evaluation function J_u and the Hamiltonian can be expressed as

$$J_u = \int_0^1 \left(\frac{1}{2} T_1 \delta_1^2 + \frac{1}{2} T_2 \delta_2^2 \right) d\tau, \tag{23}$$

$$H = T_1 \left(\frac{1}{2}\delta_1^2 + \lambda_{x1} v_1 + \lambda_{v1} a_1 + \lambda_{a1} \delta_1 \right) + T_2 \left(\frac{1}{2}\delta_2^2 - \lambda_{x2} v_2 - \lambda_{v2} a_2 - \lambda_{a2} \delta_2 \right). \tag{24}$$

The necessary conditions for minimizing the evaluation function J_u are given as follows:

$$\acute{\boldsymbol{\lambda}} = -\frac{\partial H}{\partial \boldsymbol{x}}, \tag{25}$$

http://dx.doi.org/10.1016/j.robot.2017.03.010

$$\frac{\partial H}{\partial \boldsymbol{u}} = \mathbf{0}. \tag{26}$$

Accordingly, the following conditions are derived as:

$$\begin{cases} \acute{\lambda}_{x1} = 0 \\ \acute{\lambda}_{x2} = 0, \end{cases} \quad \begin{cases} \acute{\lambda}_{v1} = -T_1 \lambda_{x1} \\ \acute{\lambda}_{v2} = T_2 \lambda_{x2}, \end{cases} \quad \begin{cases} \acute{\lambda}_{a1} = -T_1 \lambda_{v1} \\ \acute{\lambda}_{a2} = T_2 \lambda_{v2}, \end{cases} \tag{27}$$

with

$$\begin{cases} \dfrac{\partial H}{\partial \delta_1} = \delta_1 + \lambda_{a1} = 0 \\ \dfrac{\partial H}{\partial \delta_2} = \delta_2 - \lambda_{a2} = 0. \end{cases} \tag{28}$$

The boundary conditions are given by the following equations from Eq. (7) as:

$$\boldsymbol{\chi} = [x_1, v_1, a_1, x_2, v_2, a_2]^T = \mathbf{0}, \tag{29}$$

$$\boldsymbol{\psi} = \begin{bmatrix} x_1 - \frac{4}{5\pi}\Theta_d^* \\ v_1 - V_d^* \\ a_1 \\ x_2 - \frac{4}{5\pi}\Theta_d^* \\ v_2 - V_d^* \\ a_2 \end{bmatrix} = \mathbf{0}. \tag{30}$$

A reference motion for target-hitting task can be computed by solving the aforementioned differential equations by using the pseudo-Newton method.

References

[1] H. Heuer, J. Lüttgen, Robot assistance of motor learning: A neuro-cognitive perspective, Neurosci Biobehav Rev 56 (2015) 222–240.

[2] P. G. Morasso, Spatial control of arm movements, Exp Brain Res 42 (1981) 223–227.

[3] T. Flash, N. Hogan, The coordination of arm movements: An experimentally confirmed mathematical model, J Neurosci 5 (7) (1985) 1688–1703.

[4] Y. Uno, M. Kawato, R. Suzuki, Formation and control of optimal trajectory in human multijoint arm movement, Biolo Cybern 61 (2) (1989) 89–101.

[5] P. Morasso, V. Sanguineti, T. Tsuji, A dynamical model for the generator of curved trajectories, in: Proceedings of the International Conference on Artificial Neural Networks, Vol. 394, 1993, pp. 115–118.

[6] T. Tsuji, Y. Tanaka, P. G. Morasso, V. Sanguineti, M. Kaneko, Bio-mimetic trajectory generation of robots via artificial potential field with time base generator, IEEE Trans Sys Man Cybern: Part C 32 (4) (2002) 426–439.

[7] Y. Tanaka, T. Tsuji, V. Sanguineti, P. G. Morasso, Biomimetic trajectory generation using a neural time base generator, J Robot Sys 22 (11) (2005) 625–637.

[8] T. Tsuji, Y. Tanaka, M. Kaneko, H. Miyaguchi, A biomimetic rehabilitation aid for reaching movements using time base generator, Mach Int Robot Cont 2 (4) (2000) 141–149.

[9] H. I. Krebs, J. J. Palazzolo, L. Dipietro, M. Ferraro, J. Krol, K. Rannekleiv, B. T. Volpe, N. Hogan, Rehabilitation robotics: performance based progressive robot-assisted therapy, Auto Robot 15 (7).

[10] V. Huang, W. Krakauer, Robotic neurorehabilitation: a computational motor learning perspective, J NeuroEng Rehab 6 (5) (2009) 1–13.

[11] L. Marchal-Crespo, M. van Raai, G. Rauter, P. Wolf, R. Riener, The effect of haptic guidance and visual feedback on learning a complex tennis task, Exp Brain Res 231 (2013) 277–291.

[12] P. S. Lum, S. L. Lehman, D. J. Reinkensmeyer, The bimanual lifting rehabilitator: An adaptive machine for therapy of stroke patients, IEEE Trans Rehab Eng 3 (2) (1995) 166–173.

[13] S. Okada, T. Sakaki, R. Hirata, Y. Okajima, S. Uchida, Y. Tomita, Tem: a therapeutic exercise machine for the lower extremities of spastic patients, Advanced Robotics 14 (7) (2001) 597–606.

[14] J. Lüttgen, H. Heuer, The influence of haptic guidance on the production of spatio-temporal patterns, Hum Mov Sci 31 (2012) 519–528.

[15] Y. Tanaka, Robot-aided rehabilitation methodology for enhancing movement smoothness by using a human hand trajectory generation model with task-related constraints, J Hum Robot Interact 4 (3) (2015) 101–119.

[16] L. Marchal-Crespo, D. J. Reinkensmeyer, Review of control strategies for robotic movement training after neurologic injury, J NeuroEng Rehab 6 (2009) doi:10.1186/1743–0003–6–20.

[17] L. E. Kahn, P. S. Lum, W. Z. Rymer, D. J. Reinkensmeyer, Robot-assisted movement training for the stroke-impaired arm: Does it matter what the robot does?, J Rehab Res Dev 43 (5) (2010) 619–630.

[18] J. L. Patton, F. A. Mussa-Ivaldi, Robot-assisted adaptive training: custom force fields for teaching movement patterns, IEEE Trans Biomed Eng 51 (4) (2004) 636–646.

[19] M. H. Milot, L. Marchal-Crespo, C. S. Green, S. C. Cramer, D. J. Reinkensmeyer, Comparison of error-amplification and haptic-guidance training techniques for learning of a timing-based motor task by healthy individuals, Exp Brain Res 201 (2010) 119–131.

[20] N. Hogan, Impedance control: an approach to manipulation: Parts i, ii, iii, ASME J Dyn Sys, Meas, Cont 107 (1) (1985) 1–24.

[21] F. Lacquaniti, C. Maioli, The role of preparation in tuning anticipatory and reflex responses during catching, Vision Res 9 (18) (1989) 134–148.

[22] M. Zago, G. Bosco, V. Maffei, M. Iosa, Y. P. Ivanenko, F. Lacquaniti, Internal models of target motion: Expected dynamics overrides measured kinematics in timing manual interceptions, J Neurophysiol 91 (2004) 1620–1634.

[23] G. Bosco, S. D. Monache, F. Lacquaniti, Catching what we can't see: Manual interception of occluded fly-ball trajectories, PLoSE ONE 7 (11) (2012) e49381.

[24] E. Brenner, J. B. J. Smeets, Hitting moving targets: Co-operative control of 'when' and 'where', Hum Mov Sci 15 (1) (1996) 39–53.

[25] H. Katsumata, D. M. Russell, Prospective versus pre-

http://dx.doi.org/10.1016/j.robot.2017.03.010

dictive control in timing of hitting a falling ball, Exp Brain Res 216 (1) (2012) 499–514.
[26] E. Brenner, B. Driesen, J. B. J. Smeets, Precise timing when hitting falling balls, Front Hum Neurosci 8 (2015) Article 342.
[27] M. Sampei, K. Furuta, On time scaling for nonlinear systems: Application to linearization, IEEE Trans on Auto Cont AC-31 (5) (1986) 459–462.
[28] R. Ihaka, R. Gentleman, R: A language for data analysis and graphics, J Comp Graphic Stat 5 (3) (1996) 299–314. URL: www.r–project.org.
[29] R. Shadmehr, F. A. Mussa-Ivaldi, Adaptive representation of dynamics during learning of a motor task, J Neurosci 14 (1994) 3208–3224.
[30] D. Wolpert, R. Miall, M. Kawato, Internal models in the cerebellum, Trends Cog Sci 2 (9) (1998) 338–347.
[31] M. Kawato, Internal models for motor control and trajectory planning, Curr Opin Neurobiol 9 (1999) 718–727.
[32] H. Imamizu, S. Miyauchi, T. Tamada, Y. Sasaki, T. Takino, B. Puetz, T. Yoshioka, M. Kawato, Human cerebellar activity reflecting an acquired internal model of a novel tool, Nature 403 (2000) 192–195.
[33] R. B. Ivry, S. W. Keele, H. C. Diener, Dissociation of the lateral and medial cerebellum in movement timing and movement execution, Exp Brain Res 73 (1) (1988) 167–180.
[34] C. Voelcker-Rehage, Motor-skill learning in older adults -a review of studies on age-related differences, Exp. Brain Res. 5 (2008) 5–16.
[35] N. Inui, Simple reaction times and timing of serial reactions of middle-aged and old men, Percept Mot Skills 84 (1997) 219–225.
[36] V. Porciatti, A. Fiorentini, M. C. Morrone, D. C. Burr, The effects of ageing on reaction times to motion onset, Vision Res. 39 (1999) 2157–2164.
[37] F. A. Mussa-Ivaldi, N. Hogan, E. Bizzi, Neural, mechanical, and geometric factors subserving arm posture in humans, J Neurosci 5 (10) (1986) 2732–2743.
[38] T. Tsuji, Y. Takeda, Y. Tanaka, Analysis of mechanical impedance in human arm movements using a virtual tennis system, Biolo Cybern 91 (5) (2004) 295–305.
[39] T. E. Milner, D. W. Franklin, Impedance control and internal model use during the initial stage of adaptation to novel dynamics in humans, J Physiol 567 (2) (2005) 651–664.

Yoshiyuki Tanaka received his B.E. degree in Computer Science and Systems Engineering from Yamaguchi University in 1995, and his M.E. and Dr. of Engineering degrees in Information Engineering from Hiroshima University in 1997 and 2001, respectively. He was a Research Associate with the Faculty of Information Sciences, Hiroshima City University from 2001 to 2002, and an Assistant Professor in the Department of Artificial Complex Systems Engineering at Hiroshima University from 2002 to 2013. He is currently an Associate Professor with the Graduate School of Engineering at Nagasaki University. His research interests include human motor control mechanism and its application to human-machine humanmachine systems. Dr. Tanaka is a member of the Robotics Society of Japan, the Japan Ergonomics Society, the Japan Society of Mechanical Engineers, the Society of Instrumentation and Control Engineers in Japan, and the Institute of Electrical and Electronics Engineers.